External light activates hair follicle stem cells through eyes via an ipRGC–SCN–sympathetic neural pathway

Sabrina Mai-Yi Fan[a], Yi-Ting Chang[b], Chih-Lung Chen[a,c], Wei-Hung Wang[a], Ming-Kai Pan[d,e], Wen-Pin Chen[f], Wen-Yen Huang[a], Zijian Xu[g], Hai-En Huang[a], Ting Chen[g], Maksim V. Plikus[h,i], Shih-Kuo Chen[b,j,1], and Sung-Jan Lin[a,c,j,k,l,1]

[a]Institute of Biomedical Engineering, College of Medicine and College of Engineering, National Taiwan University, 100 Taipei, Taiwan; [b]Department of Life Science, College of Life Science, National Taiwan University, 106 Taipei, Taiwan; [c]Department of Dermatology, National Taiwan University Hospital and College of Medicine, 100 Taipei, Taiwan; [d]Department of Medical Research, National Taiwan University Hospital, 100 Taipei, Taiwan; [e]Department of Neurology, National Taiwan University Hospital, 100 Taipei, Taiwan; [f]Institute of Pharmacology, College of Medicine, National Taiwan University, 100 Taipei, Taiwan; [g]National Institute of Biological Sciences, 102206 Beijing, China; [h]Center for Complex Biological Systems, University of California, Irvine, CA 92697; [i]Department of Developmental and Cell Biology, Sue and Bill Gross Stem Cell Research Center, University of California, Irvine, CA 92697; [j]Research Center for Developmental Biology and Regenerative Medicine, National Taiwan University, 100 Taipei, Taiwan; [k]Graduate Institute of Clinical Medicine, College of Medicine, National Taiwan University, 100 Taipei, Taiwan; and [l]Molecular Imaging Center, National Taiwan University, 100 Taipei, Taiwan

Edited by Robert J. Lucas, University of Manchester, Manchester, United Kingdom, and accepted by Editorial Board Member Jeremy Nathans June 7, 2018 (received for review November 9, 2017)

Changes in external light patterns can alter cell activities in peripheral tissues through slow entrainment of the central clock in suprachiasmatic nucleus (SCN). It remains unclear whether cells in otherwise photo-insensitive tissues can achieve rapid responses to changes in external light. Here we show that light stimulation of animals' eyes results in rapid activation of hair follicle stem cells with prominent hair regeneration. Mechanistically, light signals are interpreted by M1-type intrinsically photosensitive retinal ganglion cells (ipRGCs), which signal to the SCN via melanopsin. Subsequently, efferent sympathetic nerves are immediately activated. Increased norepinephrine release in skin promotes hedgehog signaling to activate hair follicle stem cells. Thus, external light can directly regulate tissue stem cells via an ipRGC–SCN autonomic nervous system circuit. Since activation of sympathetic nerves is not limited to skin, this circuit can also facilitate rapid adaptive responses to external light in other homeostatic tissues.

melanopsin | circadian rhythm | sympathetic nerve | hair follicle | stem cell

Adult stem cells (SCs) reside in designated niches that tightly regulate them via short-range signals (1). In complex multicellular animals such as mammals, SCs often respond to external cues while insulated from the harsh outer environment (1, 2). For such responses, pathways for detecting and precisely relaying external signals to internal SC niches must exist. Light is an important environmental signal that can modulate cell and tissue activities (1, 2). External light primarily regulates daily tissue rhythmic activities by entraining the central circadian clock located in the suprachiasmatic nucleus (SCN) through the eyes (2–4). The central circadian clock synchronizes the oscillatory activities in peripheral tissues to regulate different physiological functions and help the organism adapt to daily regular environmental changes (2).

Photoentrainment of the central circadian clock is mediated by a group of atypical photoreceptor cells named "intrinsically photosensitive retinal ganglion cells" (ipRGCs) located in the inner layer of the retina which express the photopigment melanopsin (3–7). By integrating the intrinsic melanopsin photodetection pathway and extrinsic input from rod and cone signaling, ipRGCs provide environmental luminance signals for several important non–image-forming functions, such as circadian photoentrainment, pupillary light reflex, alertness, and phototaxis (5, 6, 8–11). Compared with cone opsins and rhodopsin of rods, melanopsin requires higher light intensity for activation due to its lower density on the ipRGC cell surface and has maximum sensitivity in the short-wavelength blue light range (peak absorption ∼480 nm) (5, 12, 13). Furthermore, unlike the quick on/off signaling from cone opsins and rhodopsin in response to light, melanopsin signaling in ipRGCs can produce sustained light signals for a long period of time and has prolonged activation after the light stimulation is turned off (3, 13). In mouse retina, there are at least five subtypes of ipRGCs (M1–M5) with distinct morphological and electrophysiological properties and preferential projections to different brain regions (14–20). Specifically, M1 ipRGCs, which do not express the transcriptional factor Brn3b, innervate the SCN for circadian photoentrainment (9). Most Brn3b-positive and non-M1 ipRGCs innervate other brain regions, such as the olivary pretectal nucleus for pupillary light reflex (9). In addition to modulating animal behavior through the circadian clock, ipRGCs innervate many brain regions in the thalamus and hypothalamus (21). It is unclear whether and how ipRGCs regulate other cellular activities in peripheral tissues.

Skin is a large peripheral organ densely populated by SCs. It contains a huge number of hair follicles (HFs) that undergo

Significance

Intrinsically photosensitive retinal ganglion cells (ipRGCs) exhibit several important functions including the circadian photo entrainment, pupillary light reflex, alertness, and phototaxis. Whether ipRGCs regulate other physiological activities is unknown. We show that external light stimulation can activate hair follicle stem cells through the eyes via an ipRGC–suprachiasmatic nucleus–sympathetic nervous circuit. Immediately after ipRGCs are stimulated by light, the systemic sympathetic activities are activated. In skin, the local release of norepinephrine activates hair follicle stem cells. This neural circuit enables prompt communication between peripheral tissues and the external environment. Due to the systemic activation of sympathetic activities, this circuit can also allow for timely responses to external light in other organs. It also highlights a function of ipRGCs in regulating autonomic nervous activity.

Author contributions: S.M.-Y.F., Y.-T.C., S.-K.C., and S.-J.L. designed research; S.M.-Y.F., Y.-T.C., C.-L.C., W.-H.W., M.-K.P., W.-P.C., W.-Y.H., Z.X., and H.-E.H. performed research; T.C. and M.V.P. contributed new reagents/analytic tools; S.M.-Y.F., Y.-T.C., C.-L.C., M.-K.P., W.-P.C., T.C., M.V.P., S.-K.C., and S.-J.L. analyzed data; and S.M.-Y.F., M.V.P., S.-K.C., and S.-J.L. wrote the paper.

The authors declare no conflict of interest.

This article is a PNAS Direct Submission. R.J.L. is a guest editor invited by the Editorial Board.

Data deposition: The data reported in this paper have been deposited in the Gene Expression Omnibus (GEO) database, https://www.ncbi.nlm.nih.gov/geo (accession no. GEO: GSE98668).

[1]To whom correspondence may be addressed. Email: alenskchen@ntu.edu.tw or drsjlin@ntu.edu.tw.

This article contains supporting information online at www.pnas.org/lookup/suppl/doi:10.1073/pnas.1719548115/-/DCSupplemental.

Published online June 29, 2018.

repetitive cycles of regeneration consisting of growth (anagen), regression (catagen), and rest (telogen) phases (22). Activation of each new regeneration cycle is fueled by HF stem cells (HFSCs) residing in the so-called "bulge" and "secondary hair germ" niche compartments (23, 24). When HFSC activity is suppressed, entrance to anagen is prohibited (25–29). HFSC activity has been shown to be regulated by intrinsic intracellular factors as well as by the signals from the local and systemic environments (1, 26, 30–35). In addition to these internal regulatory factors, HF regeneration can be altered by external cues (1, 36). Therefore, HFs provide an opportunity for interrogating the mechanisms by which tissue SCs communicate with the outer environment and how changes in the external environment are perceived and transmitted to an internal SC niche. Using the HF regeneration paradigm, we uncovered a noncircadian neural circuit that activates HFSCs in response to light stimulation through retinal ipRGCs.

Results

Visible Light Stimulation to Eyes Induces Hair Regeneration. In mice, the second telogen in back skin lasts for ∼6 wk starting from week 7 of age (22) (Fig. 1*A*). To test whether ocular light stimulation can influence HF regeneration, 7-wk-old C57BL/6 mice (n = 10) were exposed daily to blue light stimulation (463 ± 50 nm, 4 mW/cm^2 or 9.32 × 10^{15} photons·cm^{-2}·s^{-1}; 2 J/cm^2 for 8 min and 20 s) to the eyes under anesthesia for 10 consecutive days at zeitgeber time (ZT)1–2 (1–2 h after light-on during the daily light/dark cycle) (Fig. 1*A*). During light stimulation, only the animal's head was exposed with the eyes kept open. Activation of a new anagen phase, marked by prominent darkening of the skin due to pigment production in anagen HFs (22, 26), was observed between day 5 and day 11 after the initial light stimulation (Fig. 1 *B* and *C*). Consistently, regions of new hair growth first appeared simultaneously on both sides of the trunk and extended toward the central back (Fig. 1*B*). Such patterns are distinct from the largely synchronized hair growth on the whole back during the second physiological cycle (22), and also are different from the pattern of hair regrowth induced by direct light irradiation to the dorsal skin that first appeared homogenously on the back and then extended to the lateral trunk (*SI Appendix*, Fig. S1*D*) (37). Skin of unirradiated control mice remained in telogen phase for more than 21 d (n = 10) (Fig. 1 *B* and *C*). We also irradiated mice without anesthesia and found that mice became agitated and tried to avoid intense light, thus reducing the light stimulation to eyes. In this condition, anagen entry could be induced by increasing the daily blue light irradiation (6 J/cm^2 or 9.32 × 10^{15} photons·cm^{-2}·s^{-1} for 25 min) (*SI Appendix*, Fig. S1*C*). To provide a consistent amount of light exposure among animals, we irradiated mice under anesthesia for all the following experiments.

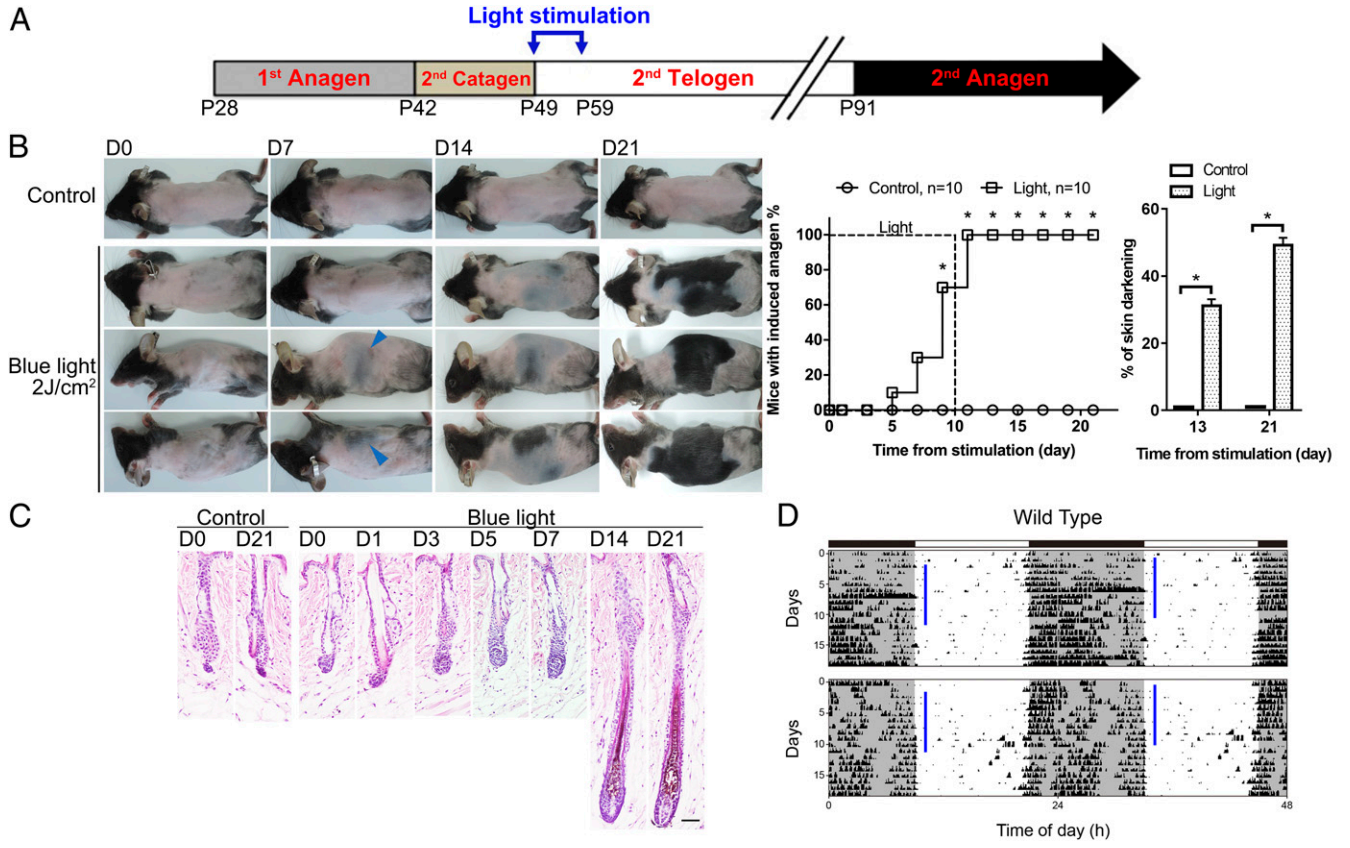

Fig. 1. Optic blue light stimulation promotes anagen entry without changing the ongoing circadian rhythm. (*A*) Postnatal mouse hair cycle and light stimulation. Daily light stimulation to the eyes was initiated on postnatal day 49 for 10 consecutive days. (*B*) Effect of daily optic blue light irradiation (463 ± 50 nm, 2 J/cm^2) on anagen entry. Successful induction of anagen was defined as more than 10% of the dorsal skin turning from pink to gray/black or with hair emergence. Anagen was first induced on sides of the trunk (blue arrowheads) and extended toward the central back. No hair regrowth was observed in unirradiated control mice. Dorsal skin with anagen entry (percentage of skin darkening) was significantly higher in the irradiated group on both day 13 and day 21. *P < 0.05 (n = 10). (*C*) Histology. Under blue light stimulation, premature anagen entry was induced, and HFs started to enlarge and elongate from day 3. In unirradiated control mice, HFs remained in telogen. (Scale bar, 50 μm.) (*D*) Effect of daily optic blue light stimulation on the ongoing circadian rhythm. The ongoing circadian rhythm was not changed by daily blue light stimulation. Similar results were obtained in five independent experiments. Vertical blue bars indicated the time of light irradiation each day.

Next, we titrated doses of light and also compared blue light with green light (522 ± 50 nm, 2 J/cm^2 or 7.88 × 10^{15} photons·cm^{-2}·s^{-1} for 11 min 7 s). We found that green light also induced hair growth, albeit less effectively, and that both spectra produced dose-dependent responses in hair regeneration (*SI Appendix*, Fig. S1 *A* and *B*). At a lower amount of photons, 0.5 J·cm^{-2}·d^{-1}, only blue light (9.32 × 10^{15} photons·cm^{-2}·s^{-1} for 2 min 5 s), but not green light (7.88 × 10^{15} photons·cm^{-2}·s^{-1} for 2 min 47 s), could induce anagen entry (*SI Appendix*, Fig. S1*B*). These results showed that mice were more sensitive to short-wavelength blue light than to long-wavelength green light for hair regeneration promotion. To clarify whether light irradiation to the eyes changes the central circadian clock, we recorded the daily activities of mice. Locomotion tests showed that animals' daily activity rhythms were not significantly changed under blue light stimulation (Fig. 1*D*).

Intact Optic Nerves but Not Cones/Rods Are Required for Light-Triggered Hair Regeneration. To confirm that the signal for HF regeneration originates from the retina, optic nerves were crushed before light stimulation. This completely abolished hair growth induction ($n = 10$) (Fig. 2*A* and *SI Appendix*, Fig. S2*A*) and suggested that retinal photoreceptors and neural circuits are essential for the light-triggered HF regeneration. Next, we evaluated the involvement of retinal photoreceptors, rods, and cones vs. ipRGCs (5). We irradiated *Gnat1*$^{-/-}$; *Gnat2*$^{cpfl3/cpfl3}$ mice, whose light signal transduction from rods and cones was disrupted (38, 39). Accelerated hair growth was still induced in light-treated mutant mice ($n = 10$), albeit more slowly and with a reduced area of hair regrowth in comparison with wild-type animals (Fig. 2*B* and *SI Appendix*, Fig. S2*B*). These results showed that, while rod and cone cells might play a minor role in light-triggered hair regeneration, neural projection of retinal ganglion cells to the brain is required.

Light Accelerates Hair Regeneration Through Melanopsin and the ipRGC-to-SCN Projection. In addition to rod and cone cells, ipRGCs are the third type of photoreceptor cells in the eyes (4, 5). Since melanopsin is the photoreceptor molecule for ipRGCs (4, 5), we tested whether melanopsin is required for light-induced HF regeneration by exposing mice null for melanopsin (*Opn4*$^{-/-}$ mice) to daily blue light stimulation. *Opn4*$^{-/-}$ mice ($n = 10$) did not exhibit premature hair cycle entry under blue light stimulation (Fig. 3*A* and *SI Appendix*, Fig. S3). These results support the notion that melanopsin in ipRGCs is essential and sufficient for light-induced hair growth.

In mouse retina, there are at least five subtypes of ipRGCs preferentially projecting to distinct brain regions (14). To determine which subtype of ipRGCs conveys light signals for HF regeneration, we light-treated *Opn4*$^{Cre/+}$; *Brn3b*$^{Z\text{-}dta/+}$ mice whose SCN-targeting M1 ipRGCs were preserved while non-M1 ipRGCs were ablated (9). *Opn4*$^{Cre/+}$; *Brn3b*$^{Z\text{-}dta/+}$ mice ($n = 10$) still maintained accelerated HF regeneration (Fig. 3*B* and *SI Appendix*, Fig. S4), although anagen induction was a bit slower and reduced in comparison with wild-type mice. We also irradiated *Opn4*$^{dta/+}$ mice, whose M1 ipRGCs were mostly ablated at 7 wk of age (*SI Appendix*, Fig. S5*A*) (40). Because *Opn4*$^{dta/+}$ mice might have attenuated circadian photoentrainment, we monitored their daily locomotion activity onset and light-treated them at circadian time (CT) 1 (*SI Appendix*, Fig. S5*B*). Compared with wild-type controls ($n = 5$), light-induced hair growth was significantly delayed and reduced in *Opn4*$^{dta/+}$ mutants ($n = 5$) (Fig. 3*C* and *SI Appendix*, Fig. S5*C*). Together, our results suggest that M1 cells are the predominant ipRGCs for conveying external light information to the SCN for hair cycle activation.

Ocular Light Stimulation Activates Systemic Sympathetic Activities and Promotes Hair Regeneration by Increasing Cutaneous Norepinephrine Release. It has been shown that SCN can signal to peripheral tissues through the hypothalamic–pituitary–adrenal pathway or the

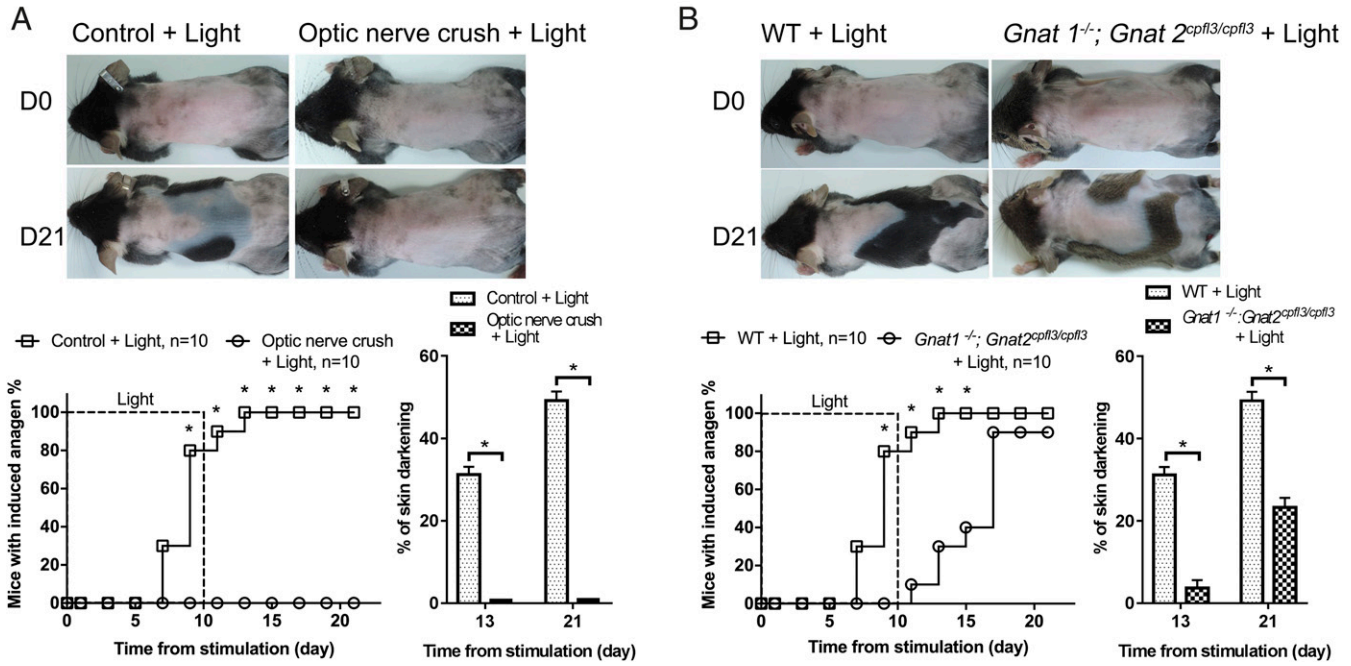

Fig. 2. Intact optic nerves are essential for light-triggered anagen entry. (*A*) Effect of optic nerve crushing. Premature anagen induction by blue light was completely prohibited after optic nerves were disrupted. *$P < 0.05$ ($n = 10$). (*B*) Roles of rods and cones. Anagen entry could still be induced by light in *Gnat1*$^{-/-}$; *Gnat2*$^{cpfl3/cpfl3}$ mice whose signaling from rods and cones was inactivated, but the area with anagen induction was reduced in comparison with wild-type mice. *$P < 0.05$ ($n = 10$).

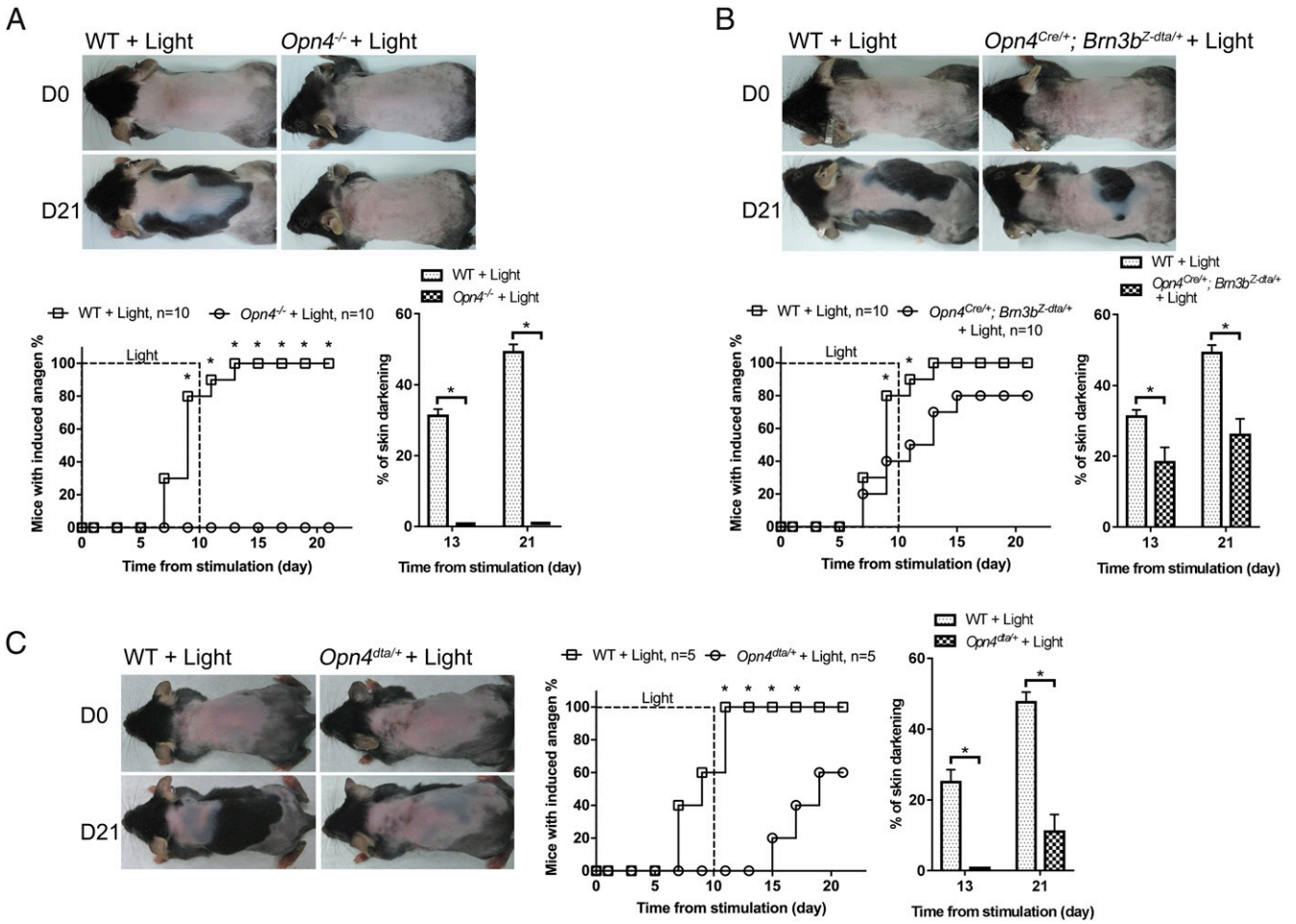

Fig. 3. Light triggers anagen entry through melanopsin and the ipRGC-to-SCN projection. (*A*) Effect of *Opn4* deletion. Light-induced anagen entry was completely abolished in $Opn4^{-/-}$ mice. $^*P < 0.05$ ($n = 10$). (*B*) Effect of depleting $Brn3b^+$ ipRGCs. Anagen could still be induced in $Opn4^{Cre/+}$; $Brn3b^{Z\text{-}dta/+}$ mice, but light-induced anagen entry was slightly delayed and reduced in $Opn4^{Cre/+}$; $Brn3b^{Z\text{-}dta/+}$ mice compared with wild-type mice. $^*P < 0.05$ ($n = 10$). (*C*) Effect of reduced neuronal input from ipRGCs. Reduced ipRGC numbers in $Opn4^{dta/+}$ mice delayed and reduced light-induced anagen entry. $^*P < 0.05$ ($n = 5$).

sympathetic nervous system (41, 42). Whether light stimulation to ipRGCs can immediately alter the activity of the systemic endocrine or the sympathetic nervous system is unknown. We examined whether signaling relay to HFs is mediated by systemic circulating factors. We generated parabiotic mice and illuminated the eyes of only one of the two paired animals. We confirmed the successful establishment of parabiosis by i.v. injecting a fluorescent dye in one mouse and detecting the fluorescence in the paired mouse before light irradiation. Accelerated hair growth was induced only in light-treated ($n = 5$) mice, but not in conjoint nontreated mice ($n = 5$) (Fig. 4*A*). It was shown that circulatory prolactin and melatonin might regulate HF growth (43–46). We found that, compared with control mice, only melatonin was slightly reduced 50 min after light exposure when mice were irradiated at ZT1–2 (*SI Appendix*, Fig. S6*A*). The results suggest that circulatory factors might not play a major role in light-induced HF regeneration.

Autonomic nerves regulate many cellular activities in peripheral tissues (47–49). Consistent with previous reports (50), we found that sympathetic nerves not only innervate arrector pili muscles of the HFs (*SI Appendix*, Fig. S6*C*) but also project to the HFSC niche (Fig. 4*B* and *SI Appendix*, Fig. S6*B*). To determine whether sympathetic nerves are activated through the melanopsin photodetection system, we measured sympathetic activities in light-treated wild-type and $Opn4^{-/-}$ mice. Ocular light stimulation increased the heart rate, perspiration, and the renal sympathetic activity in wild-type mice but not in $Opn4^{-/-}$ mutants (Fig. 5 *A*–*C*). The increased heart rate and sympathetic activity continued for more than 40 min after light stimulation. With respect to HFs, light-induced hair growth was blocked when cutaneous sympathetic innervation was disrupted by 6-hydroxydopamine (6-OHDA) treatment (Fig. 4 *B* and *C* and *SI Appendix*, Fig. S6*D*). These results suggest that light stimulation to the eyes immediately activates sympathetic activities in multiple organs through a melanopsin signaling pathway from ipRGCs and promotes HF regeneration through cutaneous sympathetic nerves.

To further confirm the involvement of the cutaneous sympathetic nervous system, we quantified changes in cutaneous norepinephrine, the neurotransmitter released by peripheral sympathetic nerve endings. Five minutes after ocular illumination, norepinephrine levels increased by about 10-fold in the skin of wild-type mice but not in the skin of $Opn4^{-/-}$ mice ($n = 3$) (Fig. 5*D*). Furthermore, consistent with previous reports (50, 51), we found that HFSCs express β2-adrenergic receptors in all the HFs examined ($n = 30$) (Fig. 5*E*). We then treated skin topically with propranolol, a β-adrenergic antagonist, and found that light-induced HF regeneration was suppressed ($n = 10$) (Fig. 5*F* and *SI Appendix*, Fig. S6*E*). Together, these results reveal that

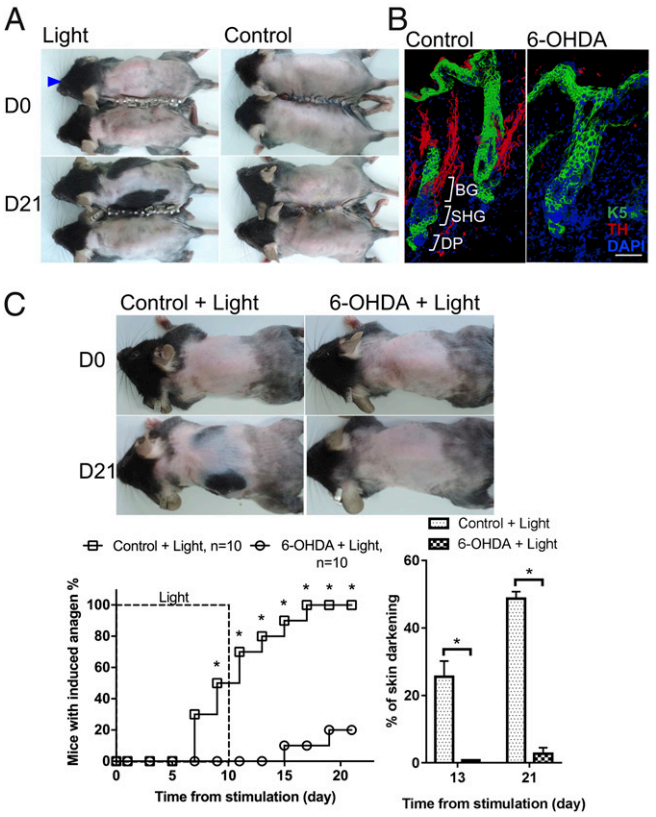

Fig. 4. Sympathetic nerves innervating HFs are required for light-induced anagen entry. (*A*) Effect of parabiosis. Light stimulation induced anagen only in the irradiated mouse (blue arrowhead) but not in the paired non-irradiated mouse. Similar results were obtained in five independent experiments. (*B*) Compressed immunostaining images of thick (34-μm) sections. (*Left*) In telogen, sympathetic nerves were in close proximity to bulge (BG) and secondary hair germ (SHG) areas before looping around arrector pili muscles. (*Right*) 6-OHDA treatment disrupted sympathetic innervation in all HFs examined ($n = 30$). DP, dermal papilla; K5, keratin 5; TH, tyrosine hydroxylase. (Scale bar, 50 μm.) (*C*) Effect of pharmacological sympathectomy with 6-OHDA. 6-OHDA treatment inhibited light-triggered anagen entry. $^*P < 0.05$ ($n = 10$).

melanopsin-dependent local norepinephrine release in skin promotes HF regeneration.

Ocular Light Irradiation Activates HFSCs by Enhancing Hedgehog Signaling. Since new anagen entry is driven by HFSC activation (23, 24), we examined how light affects HFSC quiescence. BrdU pulse-labeling showed that HFSCs started to proliferate between day 3 and 5 after initial light stimulation (Fig. 6*A*). Gene ontology analysis of whole-skin transcriptomes 1 d after the initiation of light exposure revealed that ocular light stimulation activated multiple signaling pathways (Fig. 6*B*). Hedgehog signaling and hedgehog-associated basal cell carcinoma signaling were among the top five most significantly changed ontologies (Fig. 6*B*).

During the physiological telogen-to-anagen transition, Wnt signaling, required for anagen entry, is first activated in the HFSC compartment (24, 25, 52). In telogen, there is localized hedgehog signaling activity in the upper bulge and the secondary hair germ due to hedgehog ligand production from sensory nerves surrounding the upper bulge region and from dermal papilla cells below the hair germ (53, 54). After HFs enter anagen with prominent HFSC proliferation, hedgehog signaling is highly activated in the entire HFSC population due to the enhanced production of hedgehog ligands from early transit-amplifying cells (55, 56). Although not required for the initiation of physiological anagen, the enhanced activation of hedgehog signaling early after anagen onset is essential for further growth and maturation of the lower segment of anagen HFs (55–57). We sorted HFSCs for further analysis 1 d after the initiation of light stimulation when HFSCs were still quiescent (Fig. 6*A*). We found that *Gli1* and *Gli2*, downstream targets of hedgehog signaling, were up-regulated in the HFSC compartment, including bulge SCs and hair germ SCs (Fig. 6*C*). These results showed that ocular light stimulation enhanced hedgehog signaling in HFSCs before they were activated to initiate anagen. To further test whether activation of hedgehog signaling is required for light-triggered anagen initiation, we topically administered cyclopamine, a Smoothened inhibitor, and GANT61, a Gli1/2 inhibitor. Topical treatment with cyclopamine ($n = 10$) or GANT61 ($n = 5$) inhibited light-induced HFSC activation and hair cycle entry (Fig. 6 *D* and *E* and *SI Appendix*, Fig. S7 *A* and *B*). These results suggest that hedgehog signaling is activated and required for ocular light stimulation-induced HFSC activation and anagen initiation.

Discussion

In summary, we discovered a neural circuit initiating from M1-type ipRGCs in the retina that regulates HFSC activation in response to external photic cues (Fig. 7). Since ipRGCs also contribute to the photoentrainment of the central circadian clock in the SCN (3, 4), our results demonstrate a function of ipRGCs in the immediate conveyance of the external light message to internal peripheral tissues.

In $Opn4^{-/-}$ mice and mice with crushed optic nerves, the light-induced anagen entry was completely abolished. In the mouse eyes, melanopsin is expressed only in ipRGCs and iris muscles (5, 58). Our results suggest the essential role of retinal ipRGCs in mediating the effect. The optic nerve crushing could potentially damage trigeminal nerves, and it was shown that optic nerve crushing could not completely block the activation of melanopsin-expressing trigeminal neurons (59). Our study showed that optic nerve crushing completely suppressed light-induced hair regeneration. Although it is unlikely that melanopsin-expressing trigeminal neurons are the primary photon detector for light-induced hair regeneration, we cannot completely rule out the potential contribution of this non-retinal pathway. Because light is able to promote hair regeneration in $Opn4^{Cre/+}$; $Brn3b^{Z\text{-}dta/+}$ mice in which only M1 ipRGCs (~200 cells per eye) (*SI Appendix*, Fig. S5*A*) that selectively innervate the SCN are preserved, our data suggest that M1 ipRGCs and the SCN are part of the neural circuitry that can transmit light information to alter peripheral SC activity. This mechanism is mediated through the retinohypothalamic tract that signals to the SCN to activate the sympathetic nervous system (Fig. 7). The stimulated sympathetic activity here is distinct from its daily oscillation controlled by the central circadian clock (49). Compared with the circadian clock that optimizes cellular activities in anticipation of daily rhythmic environmental changes, the circuit described here allows immediate cellular responses to external environmental cues. Since projection of ipRGCs through the retinohypothalamic tract to SCN is also essential for photoentrainment of the central circadian clock (3), our results also show the multifunctionality of the ipRGC–SCN pathway both in regulating long-term daily oscillatory activities and in relaying immediate photic information to peripheral tissues. Therefore, in addition to its known functions, we demonstrate another important role of ipRGCs in regulating physiological functions in peripheral tissues through the sympathetic nervous system. Since photoentrainment of the central circadian clock and direct optic stimulation of sympathetic activities both require the projection of ipRGCs to the SCN (60, 61), it is an intriguing question whether distinct ipRGCs or the same ipRGCs innervating SCN are employed for these two functions.

Due to the sophisticated network of both sensory and sympathetic nerves around HFs and their dynamic remodeling

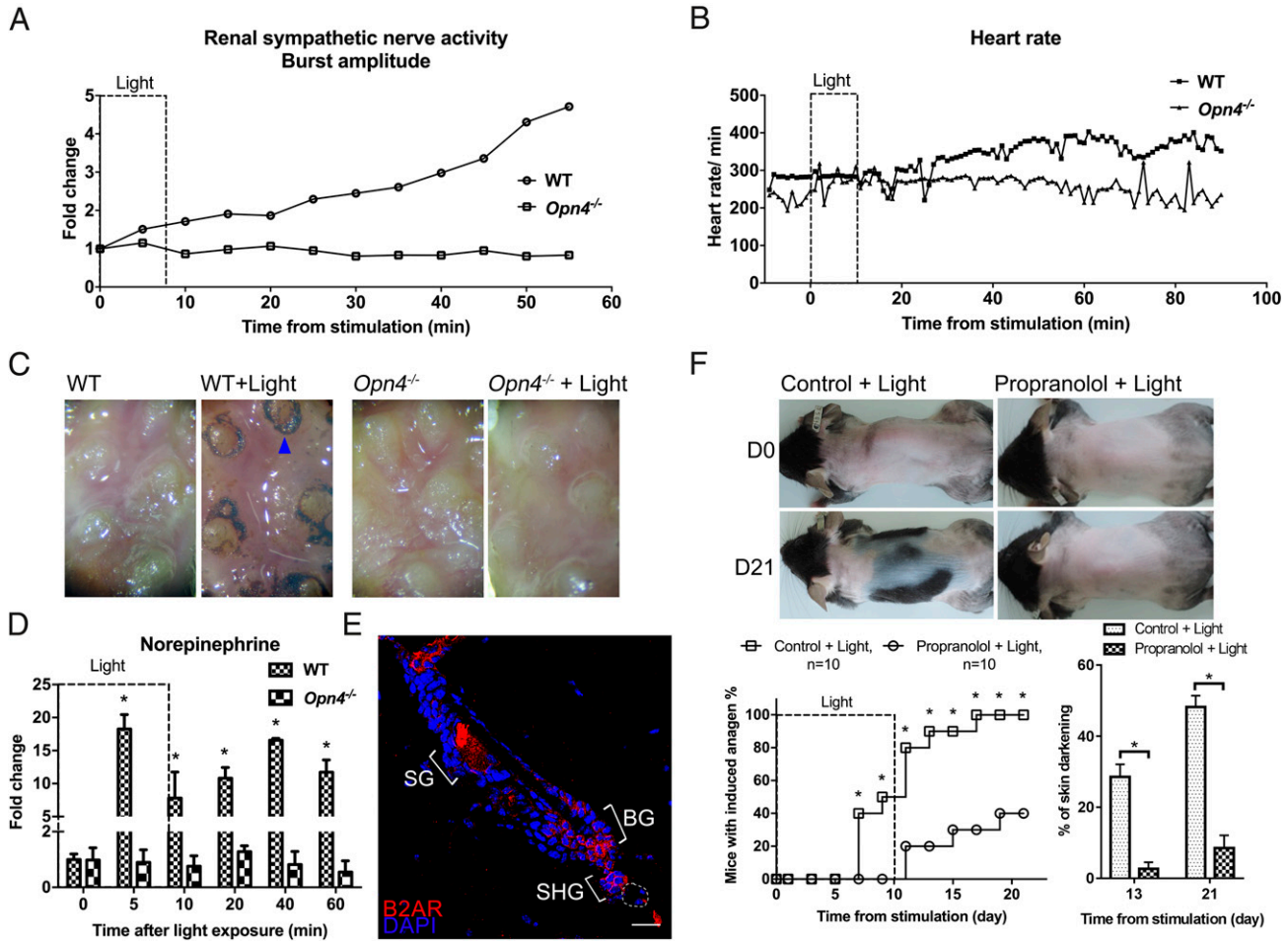

Fig. 5. Optic light stimulation activates sympathetic nerves and promotes anagen entry by enhancing norepinephrine release in skin. (*A*) Effect of light stimulation on renal sympathetic nerve activity. Sympathetic activity was increased by optic blue light stimulation in wild-type mice but not in *Opn4*$^{-/-}$ mice. Similar results were obtained in three independent experiments. (*B*) Effect of light stimulation on heart rates. The heart rate was increased by optic blue light stimulation in wild-type mice but not in *Opn4*$^{-/-}$ mice. Similar results were obtained in three independent experiments. (*C*) Effect of light stimulation on footpad sweating. Optic blue light stimulation induced sweating (blue arrowhead) in wild-type mice but not in *Opn4*$^{-/-}$ mice. Similar results were obtained in three independent experiments. (*D*) Effect of light on cutaneous norepinephrine release. Norepinephrine was highly increased after light irradiation in wild-type mice but not in *Opn4*$^{-/-}$ mice. $*P < 0.05$ compared with time 0 ($n = 3$). (*E*) Immunostaining. Enriched expression of β-2 adrenergic receptor (B2AR) in the HFSC compartment. A similar pattern of expression was observed in all HFs examined ($n = 30$). BG, bulge; SG, sebaceous gland; SHG, secondary hair germ. Dashed line represents dermal papilla. (Scale bar, 50 μm.) (*F*) Effect of β-adrenergic antagonist. Topical propranolol inhibited light-induced anagen entry. $*P < 0.05$ ($n = 10$).

around hair cycles, piloneural interactions have been suggested to be involved in regulating the physiology of HFs (50, 62, 63). However, whether the piloneural network can directly activate HFSCs for hair regeneration was unknown. Sensory nerves have been shown to densely innervate the upper bulge region of HFs and to regulate a small population of SCs in the upper bulge area by providing the ligand of sonic hedgehog (53, 62). The focally intensified hedgehog signaling in the upper bulge region defines a population of SCs that are able to become interfollicular epidermal cells upon skin wounding but is not sufficient to activate the general HFSC population to initiate a new anagen (53). Sympathetic nerves also loop around the HFSC niche when they travel from the deep dermal nervous plexus to innervate the arrector pili muscle for the piloerection function (50). Sympathetic nerves were suggested to promote HF growth after a new anagen is already initiated (50). In humans, β-blockers can induce hair loss, and defective sympathetic regulation is also associated with dysregulated hair growth (64, 65). It remained unclear whether sympathetic nerves can directly activate HFSCs. Our results show that activation of sympathetic nerves can activate HFSCs by enhancing hedgehog signaling to promote anagen entry. This also supports the findings that enhancing hedgehog signaling by forced dermal or epidermal expression of sonic hedgehog ligands or by treatment with hedgehog agonists can promote the telogen-to-anagen transition (55, 57, 66). In our other testing, we irradiated the mice at ZT5–8 and found that hair regeneration could also be induced, but the hair regeneration was a bit slower than during ZT1–2. It has been shown that intrafollicular clock activity regulates the priming state of HFSCs as well as the activity of other follicular cells and that autonomic nerves can regulate local tissue clock (67–70); the responsiveness of HFSCs to light irradiation might vary as the circadian time of light irradiation is changed. Whether sympathetic nerves regulate hedgehog signaling through modulating the local clock is to be determined. Since intense white light stimulation to eyes not only activates sympathetic nerves but also suppresses the parasympathetic activity (71, 72), it is possible that blue light here might also suppress parasympathetic activities in skin to regulate HFSC activity. In addition to neural control, HF growth is also regulated by neurohormones, such as prolactin and melatonin,

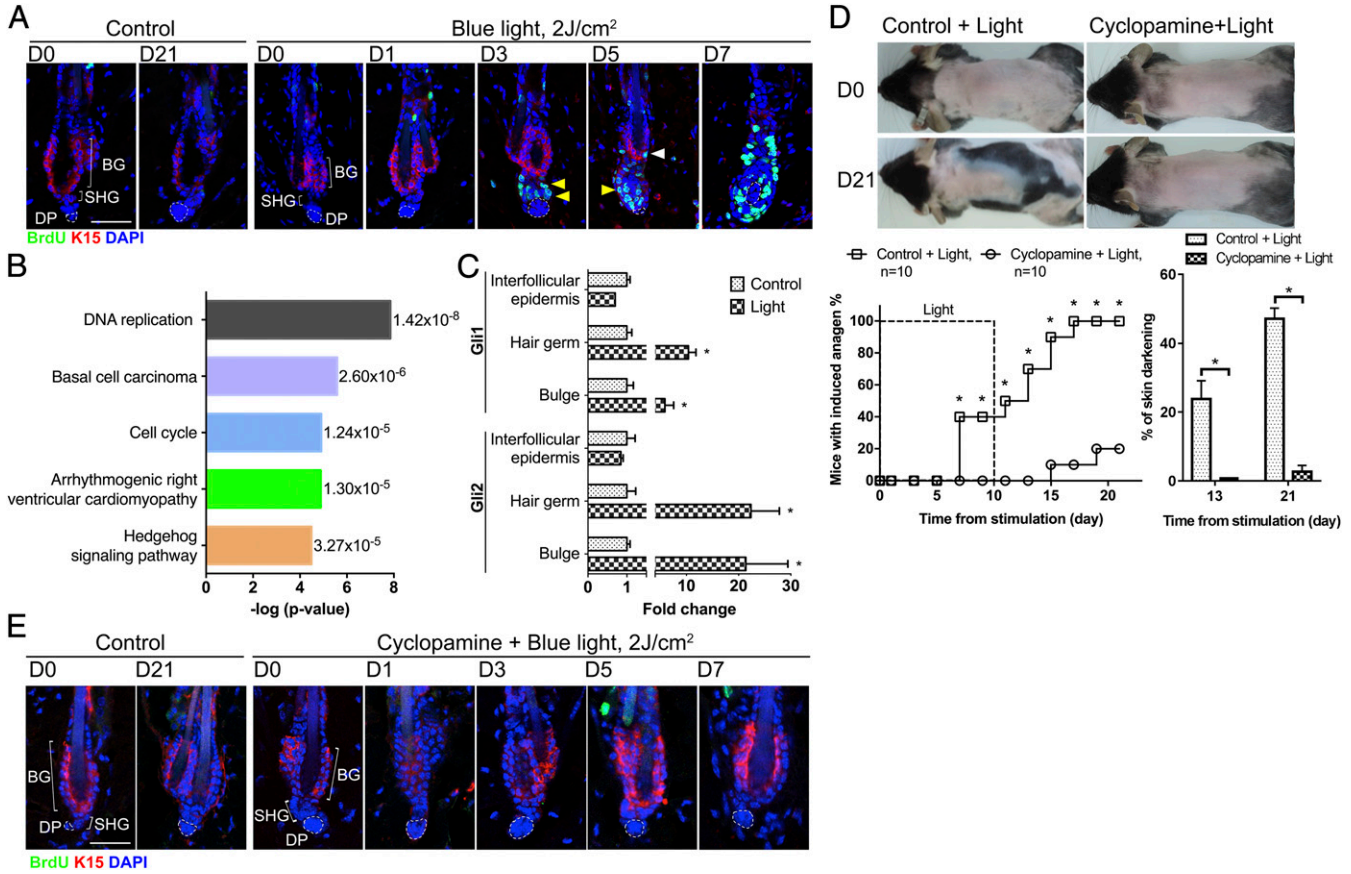

Fig. 6. Light enhances hedgehog signaling in HFSCs to promote anagen entry. (*A*) Pulse BrdU labeling under daily 2 J/cm^2 blue light stimulation. Cell proliferation of HFSCs was first observed in secondary hair germs on day 3 (yellow arrowheads) and then in the bulge area on day 5 (white arrowheads). In the nonirradiated control group, no cell proliferation was observed in the HFSC compartment. Similar results were observed in all HFs examined ($n = 30$). (Scale bar, 50 μm.) BG, bulge; DP, dermal papilla; SHG, secondary hair germ. (*B*) Analysis of gene expression 1 d after initiation of light stimulation by RNA-sequencing. The top five signaling pathways enhanced by light stimulation are shown here. *P* values are shown on the right. (*C*) Gene expression in HFSCs determined by quantitative PCR 1 d after initiation of light stimulation. Expression of *Gli1* and *Gli2* was up-regulated in bulge and secondary hair germ SCs after light irradiation. In the interfollicular epidermis, expression of *Gli1* and *Gli2* was not significantly increased. *$P < 0.05$, control vs. light-treated group ($n = 3$). (*D* and *E*) Effect of hedgehog pathway inhibitor. (*D*) Topical cyclopamine inhibited light-triggered anagen entry. *$P < 0.05$ ($n = 10$). (*E*) Pulse BrdU labeling under cyclopamine treatment. Cyclopamine inhibited light-triggered HFSC activation. Similar results were observed in all HFs examined ($n = 30$). (Scale bar, 50 μm.)

and these neurohormones can also be produced intrafollicularly (43–46). Although we did not detect extensive changes in plasma prolactin and melatonin after blue light irradiation, the intrafollicular melatonin might be changed due to the local release of noradrenaline (45, 46).

HFSCs respond to both short-range and long-range signals from the surrounding tissues and systemic environment, including HF dermal papilla cells, fibroblasts, adipose tissue, macrophages, resident regulatory T cells, neighboring HFs, and systemic hormones (1, 26, 30–35). The response of HFSCs to external light not only adds another layer to HF regeneration mechanisms but also raises a broader question with respect to the definition of SC niches. Conventionally, the SC niches have been defined as a constellation of neighboring cells and local extracellular factors that constitute the microenvironment in proximity to SCs (73). Here we show that the external environment can also regulate the internal SCs through an ipRGC–SCN–sympathetic nervous pathway. Hence, the external environment should also be considered part of the SC niche components, and internal SCs can be linked to the external component of the SC niche by the neural circuit we show here. We can consider the SC niche at three levels, i.e., the local SC microenvironment as the "microniche," the systemic environment (such as circulatory hormones) inside the body as the "macroniche," and the external environment as the "meganiche." The ipRGC–SCN–sympathetic nervous pathway enables quick regulation of tissue SCs by the meganiche through modulating the microniche.

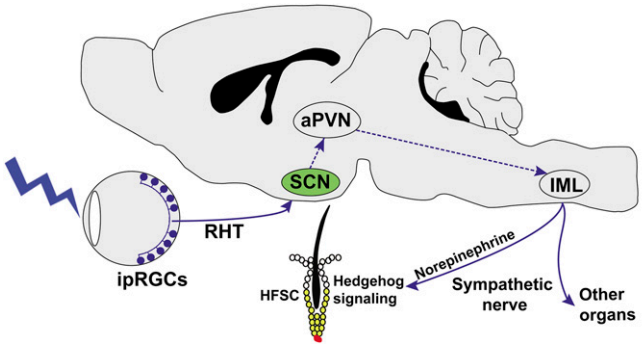

Fig. 7. Depiction of the neural pathway for light-stimulated sympathetic activity and HFSC activation. aPVN, autonomic neurons of the paraventricular nucleus; HFSC, hair follicle stem cell; IML, intermediolateral cell column; RHT, retinohypothalamic tract. Dashed lines indicate proposed neural relays for this pathway.

For animals, especially nocturnal mice, intense ambient light can be a danger signal that warrants immediate reaction. In physiological conditions, mice would not receive prolonged intense light stimulation to the eyes during the daytime unless they are threatened, such as being chased by predators or forced to move due to harsh environmental changes. Without plucking, the old mouse pelage hair within an HF is normally not shed as the new hair forms (74). Initiation of a new round of hair growth by light stimulation may make a denser hair coat for additional protection from the harsh environment or timely replenish hair accidentally lost in a stressed condition. Here we demonstrated the indirect stimulating effect of light on hair regeneration through melanopsin in ipRGCs. We have shown that direct irradiation of skin by visible light can also promote the telogen-to-anagen transition by enhancing epithelial–mesenchymal interactions and that red light is more potent than green/blue light (37). Direct irradiation to HFs also promoted hair growth in vitro (75). Hence, visible light of different spectra possesses differential direct and indirect stimulatory cues to HFSCs. In the wild, the murine body is covered by a dense hair coat, and indirect stimulation by light through the eyes would be a more prominent mechanism in the regulation of HFSCs. Although melanopsin (*Opn4*) is not expressed in HFs, rhodopsin (*Opn2*) and panopsin (or encephalopsin) (*Opn3*) are present in HFs (75). The stimulating effect of direct light irradiation to the skin may be mediated in part through nonvisual effects of these opsins (75).

Our result is consistent with previous reports showing that intense white light can alter the autonomic nervous activities in rodents (41, 71). We show that, compared with green light of a longer wavelength, blue light is more efficient in activating the ipRGC–SCN–sympathetic nervous pathway due to melanopsin's preferential absorption of light in the blue light spectrum (76). In addition to HFSCs, SCs in other tissues are also regulated by autonomic nerves (47, 49, 77, 78). The activity of tissue SCs exhibits circadian changes corresponding to the daily oscillation of autonomic nervous activities governed by the central circadian clock (49). The ability to modulate SC activities beyond its circadian changes might be applied for clinical purposes (79). Since the light-activated sympathetic activity is not limited to skin (Fig. 5 *A*–*C*) (41, 71, 72), the ipRGC–SCN–sympathetic circuit might have a role in coordinating systemic responses and hence have a broader effect on the behavior of SCs and physiological activities in other organs.

Materials and Methods

Animals. The animal experiments were approved by Animal Care and Use Committee of National Taiwan University. Female mice were used in this study. Animals were fed ad libitum and housed in animal facilities with 12-h light/12-h dark cycles. C57BL/6 mice were purchased from the Taiwan National Laboratory Animal Center. The transgenic mice *Opn4*$^{-/-}$, *Gnat1*$^{-/-}$, *Gnat2*$^{cpfl3/cpfl3}$, *Opn4*$^{Cre/+}$, *Brn3b*$^{Z\text{-}dta/+}$, and *Opn4*$^{dta/+}$ were generated with a mixed background (C57BL6; 129SvJ) and were backcrossed to C57BL/6 mice; they have been described in our prior work (9, 80). They were kindly provided by Samer Hattar (Johns Hopkins University, Baltimore). For experimental procedures, mice were anesthetized with a mixture of zolazepam (Zoletil veterinary anesthesia; Virbac Laboratories) and xylazine (Rompun; Bayer) (4:1, vol/vol) unless stated otherwise.

Light Irradiation. A tailor-made light box with light-emitting diodes of adjustable light intensity on the ceiling (Lustrous Technology Ltd.) was employed (37). Light-emitting diodes of two different wavelengths were used: blue light (463 ± 50 nm, 4 mW/cm^2 or 9.32 × 10^{15} photons·cm^{-2}·s^{-1}) and green light (522 ± 50 nm, 3 mW/cm^2 or 7.88 × 10^{15} photons·cm^{-2}·s^{-1}). Light intensity was measured by a digital light meter (DLM 530; Tecpel) at the level of the mouse eyes, and the intensity of light of each wavelength was kept constant in our experiments. The dose of light exposure was adjusted by varying the time mice spent in the light box. The temperature fluctuation within the light box was less than 1 °C during light irradiation. The dorsal skin of 7-wk-old female mice whose dorsal hair cycle was in the second telogen phase was carefully shaved first with an electric clipper (Oster Golden A5 Single Speed Animal Grooming Clipper with Oster Cryogen-X #50 Pet Clipper Blades) and then with a razor (Braun MobileShave M-60) without damaging the skin. The mice were shielded by aluminum foil from the neck to the tail to avoid light irradiation, and only the heads were exposed. The mice were in a prone position with eyes facing up toward the light-emitting diodes. Under anesthesia, their eyes opened spontaneously. The mice were exposed daily to blue light irradiation (4 mW/cm^2 or 9.32 × 10^{15} photons·cm^{-2}·s^{-1}; 8 min 20 s/d) or to green light (3 mW/cm^2 or 7.88 × 10^{15} photons·cm^{-2}·s^{-1}; 11 min 7 s/d) at 2 J/cm^2 at ZT1–2 (1–2 h after lights on during the daily light/dark cycle) for 10 consecutive days. To determine the dose effects, irradiation was reduced to 0.5 J·cm^{-2}·d^{-1} with the same light intensity. For control, mice were given the same treatment without the light on. To compare hair regrowth patterns, mice were irradiated by blue light (2 J·cm^{-2}·d^{-1}) to the dorsal skin only at ZT1–2 for 10 consecutive days, as we previously described (37). Mice were irradiated under anesthesia in our light stimulation experiments unless stated otherwise. We also irradiated the mice with blue light (6 J/cm^2 or 9.32 × 10^{15} photons·cm^{-2}·s^{-1} for 25 min) in the unanesthetized condition.

Anagen initiation was quantified by the change in skin color as we previously described (26, 37). Anagen was determined by the skin color changing from pink to gray/black (22, 26). The skin color of the mice was examined visually and photographed to determine the area of anagen entry. The proportion of the dorsal pigmented region over the entire dorsum was calculated by the software Image J (NIH; https://rsb.info.nih.gov/ij/) as we previously described (37). Successful induction of anagen entry was defined as more than 10% of the dorsal skin turning from pink to gray/black or with hair emergence from the skin.

Wheel-Running Activity. The mice were placed individually in cages with a running wheel under 12-h light/12-h dark cycles. Their activity was recorded, and the circadian period was calculated based on the ClockLab algorithm (Actimetrics). *Opn4*$^{dta/+}$ mice were given light stimulation at CT1 (circadian time) for 10 d.

Histology and Immunofluorescence. To collect skin specimens for histological analysis and immunostaining, mice were killed at different time points before and after the start of light irradiation. To gauge cell proliferation, BrdU pulse labeling was performed by i.p. injection of 10 mg/kg BrdU (Sigma-Aldrich) 1 h before mice were killed. The skin samples were fixed in 4% paraformaldehyde (PFA) (AMRESCO) in PBS AMRESCO) overnight, serially dehydrated with alcohol, and embedded in paraffin. Paraffin sections (5 μm in thickness) were stained with H&E or were prepared for immunostaining following routine procedures. Antibodies and additional details are described in *SI Appendix, SI Materials and Methods*.

Parabiosis, Nerve Crushing, Pharmacological Sympathectomy. Parabiosis was performed in 6-wk-old mice to connect them along the adjacent flanks as described (81). Their skin was connected with sutures or surgical autoclips (9-mm; Clay Adams). To confirm the successful establishment of parabiosis, one of the paired C57BL/6 mice was i.v. injected with 100 μL of fluorescent vascular imaging reagent [20 μL of Qtracker 655 (Thermo Fisher) dissolved in PBS]. Fluorescent images from the shaved dorsal side of the mice were taken by an in vivo imaging system (IVIS; Xenogen; Perkin-Elmer) at 30 and 90 min after injection. Successful parabiosis was determined by the progressive increase of fluorescence across the dorsal skin in the other of the paired mice. Only mice with confirmed successful parabiosis were used for the experiments.

To disrupt the optic nerves, optic nerves were crushed as previously described at the age of 6 wk (82, 83). The pupil light reflex was determined before and after nerve crushing, as we previously described (9). The inhibition of light reflex indicated the success of optic nerve crushing. Anterograde tracer fluorescent cholera toxin B (recombinant cholera toxin subunit B, Alexa Fluor 488 conjugate; Thermo Fisher) was also injected intravitreally to label the ganglion cells and the axons to confirm the success of optic nerve crushing (84).

Sympathectomy by s.c. injection of 10 mg/kg 6-OHDA (Tocris 2547) was performed 3 d before light stimulation (85). The 6-OHDA was divided into four equal doses in saline, which were injected into each of the four quadrants of the back. For controls, vehicle alone was used. To determine the completeness of pharmacological sympathetic denervation by 6-OHDA, the innervation of sympathetic nerves to HFs was compared in serial sections in 25–35 HFs.

Topical Drug Treatment. Propranolol (10 mg/kg body weight; Sigma P0884), cyclopamine (2 mg/kg body weight; ApexBio A8340), or GANT61 (50 mg/kg body weight; ApexBio) was dissolved in hand cream (Neutrogena Norwegian Formula Concentrated Hand Cream) at a concentration of 10 mg drug/1 g

cream. The propranolol cream, cyclopamine cream, or GANT61 cream was applied to the shaved back of mice twice a day (50 mg cream per mouse) for 10 d beginning on the first day of light irradiation. For controls, vehicle alone was used.

Heart Rate Recording. During the experiment, body temperature was maintained at 37 °C using a thermostatically regulated heating platform. Under anesthesia, heart rate and blood pressure were measured using the tail-cuff method (BP-2000 blood pressure analysis system; Visitech Systems, Inc.). The measurement was recorded at baseline for 10 min, and then the mouse eyes were exposed to blue light (2 J/cm^2, 8 min 20 s of light exposure). The recordings then lasted for 1.5 h. The control group received the same treatment without exposure to blue light.

Starch/Iodine Sweat Test. The starch/iodine method was conducted as previously described to detect sweating (86). Briefly, iodine/alcohol (2 g iodine/100 mL ethanol) was painted on the plantar surface of the rear paw. After the iodine/alcohol had dried, the rear paw surfaces were covered in a starch–oil suspension (100 g starch powder/100 mL castor oil). The mice were then irradiated with blue light (2 J/cm^2, 8 min 20 s of light exposure). After light exposure, sweating was determined by the change in skin color from brown to dark blue/black. The control group received the same treatment without exposure to blue light.

Recordings and Analysis of Renal Sympathetic Nerve Activity. To monitor sympathetic nerve activity, surgery was performed to expose the renal sympathetic nerve, and the renal sympathetic activity was recorded as previously described (87). Additional details can be found in *SI Appendix, SI Materials and Methods*.

Quantification of Cutaneous Norepinephrine Level and Plasma Prolactin and Melatonin Levels. To measure the changes of skin norepinephrine level, full-thickness mouse skin was obtained before and after light irradiation at different time points. The skin specimen was homogenized, and the norepinephrine concentration was determined by a norepinephrine ELISA kit (KA1891; Abnova) according to the manufacturer's instructions. The plasma levels of prolactin and melatonin were determined by ELISA kits for prolactin and melatonin (E-EL-M0788 and E-EL-M0083; Elabscience) according to the manufacturer's instructions. The lowest detection limits were 0.16 ng/mL for prolactin and 7.81 pg/mL for melatonin.

RNA-Sequencing and Analysis. Two hours after blue light stimulation on day 2, mouse skin was collected for RNA extraction using TRIzol reagent (Invitrogen) and the RNeasy Mini Kit (Qiagen). The cDNA was synthesized with SuperScript II reverse transcriptase (Invitrogen), and the resulting short DNA fragments were purified by the QIAquick PCR Purification Kit (Qiagen). Further sequencing and analysis are described in *SI Appendix, SI Materials and Methods*.

FACS. Bulge stem cells, hair germ stem cells, and interfollicular keratinocytes were isolated from the dorsal skin through FACS 2 h after blue light stimulation on day 2. Cells were prepared for FACS as described (88). Single-cell suspensions were then incubated with antibodies for 30 min at 4 °C. The following antibodies were employed: CD34-eFluor 660 (1:100; eBioscience); Sca1-PE-cyanine7 (1:100; eBioscience); α6-integrin-phycoerythrin (1:500; eBioscience); and CD200-FITC (1:50; Bio-Rad). Cells were sorted by a FACSAria III cell sorter (BD Biosciences). Cells were sorted as follows: bulge stem cells were Sca1$^-$/α6-integrin$^+$/CD200$^+$/CD34$^+$; hair germ stem cells were Sca1$^-$/α6-integrin$^+$/CD200$^+$/CD34$^-$; and interfollicular keratinocytes were Sca1$^+$/α6-integrin$^+$/CD200$^-$/CD34$^-$.

Real-Time PCR. Total RNA was extracted from sorted cells by TRIzol reagent (Invitrogen). cDNAs were synthesized with a RevertAid H Minus First Strand cDNA Synthesis Kit (Thermo Scientific). Quantitative real-time PCR was performed as described (89). The sequences of the primers of mouse genes were as follows: *Gapdh* (GU214026.1, 5′-CGTAGACAAAATGGTGAAGGTCGG-3′ and 5′-AAGCAGTTGGTGGTGCAGGATG-3′); *Gli1* (NM_010296.2, 5′-ATCACCTGTTGGGGATGCTGGAT-3′ and 5′-GGCGTGAATAGGACTTCCGACAG-3′); and *Gli2* (NM_001081125.1, 5′-GTTCCAAGGCCTACTCTCGCCTG-3 and 5′-CTTGAGCAGTGGAGCACGGACAT-3′).

Statistics. χ^2 test was employed for the comparison of premature anagen entry in different groups using GraphPad Prism version 5.00 (GraphPad Software). In most light-irradiation experiments, each group contained 10 mice; in some experiments, each group contained five to seven mice. Differences were considered statistically significant when the P value was <0.05. In the analysis of gene expression, data were expressed as the mean ± SEM. A two-tailed Student's t test was performed for comparisons among groups using GraphPad Prism software. A difference was considered significant when the P value was <0.05. Data were plotted using GraphPad Prism. At least two independent experiments were performed for comparisons.

ACKNOWLEDGMENTS. We thank the staff of the Eighth Core Laboratory, Department of Medical Research, National Taiwan University Hospital for technical support; Dr. Ta-Ching Chen for technical support in mouse surgery; and Drs. Sung-Tsang Hsieh, Junetai Wu, Hironobu Fujiwara, Xinhong Lim, Rejji Kuruvilla, Haiqing Zhao, and the members of the S.-J.L. laboratory for discussions. Analysis of RNA-sequencing data was performed by the Bioinformatics Core, Center of Genomic Medicine, National Taiwan University. This work was supported by the Taiwan Bio-Development Foundation (S.-J.L.); National Taiwan University Hospital Grant UN106-007 (to S.-J.L.); National Taiwan University; Taiwan Ministry of Science and Technology Grants 105-2627-M-002-010 and 103-2628-B002-004-MY3 (to S.-J.L.) and 103-2321-B-002-045 (to S.-K.C.); and an Asia-Pacific La Roche-Posay Foundation Basic Research Award (to S.-J.L.). M.V.P. is supported by a Pew Charitable Trust Grant, NIH Grants R01-AR067273 and R01-AR069653, NSF Grant DMS1763272, and Simons Foundation Grant (594598, QN).

1. Chen CC, Plikus MV, Tang PC, Widelitz RB, Chuong CM (2016) The modulatable stem cell niche: Tissue interactions during hair and feather follicle regeneration. *J Mol Biol* 428:1423–1440.
2. Janich P, Meng QJ, Benitah SA (2014) Circadian control of tissue homeostasis and adult stem cells. *Curr Opin Cell Biol* 31:8–15.
3. Berson DM, Dunn FA, Takao M (2002) Phototransduction by retinal ganglion cells that set the circadian clock. *Science* 295:1070–1073.
4. Hattar S, Liao HW, Takao M, Berson DM, Yau KW (2002) Melanopsin-containing retinal ganglion cells: Architecture, projections, and intrinsic photosensitivity. *Science* 295:1065–1070.
5. Hattar S, et al. (2003) Melanopsin and rod-cone photoreceptive systems account for all major accessory visual functions in mice. *Nature* 424:76–81.
6. Panda S, et al. (2003) Melanopsin is required for non-image-forming photic responses in blind mice. *Science* 301:525–527.
7. Provencio I, Rollag MD, Castrucci AM (2002) Photoreceptive net in the mammalian retina. This mesh of cells may explain how some blind mice can still tell day from night. *Nature* 415:493.
8. Altimus CM, et al. (2008) Rods-cones and melanopsin detect light and dark to modulate sleep independent of image formation. *Proc Natl Acad Sci USA* 105:19998–20003.
9. Chen SK, Badea TC, Hattar S (2011) Photoentrainment and pupillary light reflex are mediated by distinct populations of ipRGCs. *Nature* 476:92–95.
10. Johnson J, et al. (2010) Melanopsin-dependent light avoidance in neonatal mice. *Proc Natl Acad Sci USA* 107:17374–17378.
11. Pilorz V, et al. (2016) Melanopsin regulates both sleep-promoting and arousal-promoting responses to light. *PLoS Biol* 14:e1002482.
12. Dacey DM, et al. (2005) Melanopsin-expressing ganglion cells in primate retina signal colour and irradiance and project to the LGN. *Nature* 433:749–754.
13. Do MT, et al. (2009) Photon capture and signalling by melanopsin retinal ganglion cells. *Nature* 457:281–287.
14. Ecker JL, et al. (2010) Melanopsin-expressing retinal ganglion-cell photoreceptors: Cellular diversity and role in pattern vision. *Neuron* 67:49–60.
15. Fernandez DC, Chang YT, Hattar S, Chen SK (2016) Architecture of retinal projections to the central circadian pacemaker. *Proc Natl Acad Sci USA* 113:6047–6052.
16. Schmidt TM, Chen SK, Hattar S (2011) Intrinsically photosensitive retinal ganglion cells: Many subtypes, diverse functions. *Trends Neurosci* 34:572–580.
17. Baver SB, Pickard GE, Sollars PJ, Pickard GE (2008) Two types of melanopsin retinal ganglion cell differentially innervate the hypothalamic suprachiasmatic nucleus and the olivary pretectal nucleus. *Eur J Neurosci* 27:1763–1770.
18. Brown TM, et al. (2010) Melanopsin contributions to irradiance coding in the thalamocortical visual system. *PLoS Biol* 8:e1000558.
19. Estevez ME, et al. (2012) Form and function of the M4 cell, an intrinsically photosensitive retinal ganglion cell type contributing to geniculocortical vision. *J Neurosci* 32:13608–13620.
20. Schmidt TM, Kofuji P (2009) Functional and morphological differences among intrinsically photosensitive retinal ganglion cells. *J Neurosci* 29:476–482.
21. Hattar S, et al. (2006) Central projections of melanopsin-expressing retinal ganglion cells in the mouse. *J Comp Neurol* 497:326–349.
22. Müller-Röver S, et al. (2001) A comprehensive guide for the accurate classification of murine hair follicles in distinct hair cycle stages. *J Invest Dermatol* 117:3–15.
23. Cotsarelis G, Sun TT, Lavker RM (1990) Label-retaining cells reside in the bulge area of pilosebaceous unit: Implications for follicular stem cells, hair cycle, and skin carcinogenesis. *Cell* 61:1329–1337.
24. Greco V, et al. (2009) A two-step mechanism for stem cell activation during hair regeneration. *Cell Stem Cell* 4:155–169.
25. Choi YS, et al. (2013) Distinct functions for Wnt/β-catenin in hair follicle stem cell proliferation and survival and interfollicular epidermal homeostasis. *Cell Stem Cell* 13:720–733.

26. Plikus MV, et al. (2008) Cyclic dermal BMP signalling regulates stem cell activation during hair regeneration. *Nature* 451:340–344.
27. Chen CC, Chuong CM (2012) Multi-layered environmental regulation on the homeostasis of stem cells: The saga of hair growth and alopecia. *J Dermatol Sci* 66:3–11.
28. Kandyba E, et al. (2013) Competitive balance of intrabulge BMP/Wnt signaling reveals a robust gene network ruling stem cell homeostasis and cyclic activation. *Proc Natl Acad Sci USA* 110:1351–1356.
29. Kobielak K, Stokes N, de la Cruz J, Polak L, Fuchs E (2007) Loss of a quiescent niche but not follicle stem cells in the absence of bone morphogenetic protein signaling. *Proc Natl Acad Sci USA* 104:10063–10068.
30. Ali N, et al. (2017) Regulatory T cells in skin facilitate epithelial stem cell differentiation. *Cell* 169:1119–1129.e1111.
31. Castellana D, Paus R, Perez-Moreno M (2014) Macrophages contribute to the cyclic activation of adult hair follicle stem cells. *PLoS Biol* 12:e1002002.
32. Chen CC, et al. (2015) Organ-level quorum sensing directs regeneration in hair stem cell populations. *Cell* 161:277–290.
33. Festa E, et al. (2011) Adipocyte lineage cells contribute to the skin stem cell niche to drive hair cycling. *Cell* 146:761–771.
34. Enshell-Seijffers D, Lindon C, Kashiwagi M, Morgan BA (2010) Beta-catenin activity in the dermal papilla regulates morphogenesis and regeneration of hair. *Dev Cell* 18: 633–642.
35. Oshimori N, Fuchs E (2012) Paracrine TGF-beta signaling counterbalances BMP-mediated repression in hair follicle stem cell activation. *Cell Stem Cell* 10:63–75.
36. Maurel D, Coutant C, Boissin J (1987) Thyroid and gonadal regulation of hair growth during the seasonal molt in the male European badger, Meles meles L. *Gen Comp Endocrinol* 65:317–327.
37. Sheen YS, et al. (2015) Visible red light enhances physiological anagen entry in vivo and has direct and indirect stimulative effects in vitro. *Lasers Surg Med* 47:50–59.
38. Chang B, et al. (2006) Cone photoreceptor function loss-3, a novel mouse model of achromatopsia due to a mutation in Gnat2. *Invest Ophthalmol Vis Sci* 47:5017–5021.
39. Calvert PD, et al. (2000) Phototransduction in transgenic mice after targeted deletion of the rod transducin alpha -subunit. *Proc Natl Acad Sci USA* 97:13913–13918.
40. Chew KS, et al. (2017) A subset of ipRGCs regulates both maturation of the circadian clock and segregation of retinogeniculate projections in mice. *eLife* 6:e22861.
41. Ishida A, et al. (2005) Light activates the adrenal gland: Timing of gene expression and glucocorticoid release. *Cell Metab* 2:297–307.
42. Loewy AD (1981) Descending pathways to sympathetic and parasympathetic preganglionic neurons. *J Auton Nerv Syst* 3:265–275.
43. Kobayashi H, et al. (2005) A role of melatonin in neuroectodermal-mesodermal interactions: The hair follicle synthesizes melatonin and expresses functional melatonin receptors. *FASEB J* 19:1710–1712.
44. Foitzik K, et al. (2003) Prolactin and its receptor are expressed in murine hair follicle epithelium, show hair cycle-dependent expression, and induce catagen. *Am J Pathol* 162:1611–1621.
45. Fischer TW, Slominski A, Tobin DJ, Paus R (2008) Melatonin and the hair follicle. *J Pineal Res* 44:1–15.
46. Paus R (2016) Exploring the "brain-skin connection": Leads and lessons from the hair follicle. *Curr Res Transl Med* 64:207–214.
47. Knox SM, et al. (2010) Parasympathetic innervation maintains epithelial progenitor cells during salivary organogenesis. *Science* 329:1645–1647.
48. Jones MA, Marfurt CF (1996) Sympathetic stimulation of corneal epithelial proliferation in wounded and nonwounded rat eyes. *Invest Ophthalmol Vis Sci* 37: 2535–2547.
49. Méndez-Ferrer S, Lucas D, Battista M, Frenette PS (2008) Haematopoietic stem cell release is regulated by circadian oscillations. *Nature* 452:442–447.
50. Botchkarev VA, Peters EM, Botchkareva NV, Maurer M, Paus R (1999) Hair cycle-dependent changes in adrenergic skin innervation, and hair growth modulation by adrenergic drugs. *J Invest Dermatol* 113:878–887.
51. Steinkraus V, et al. (1996) Autoradiographic mapping of beta-adrenoceptors in human skin. *Arch Dermatol Res* 288:549–553.
52. Myung PS, Takeo M, Ito M, Atit RP (2013) Epithelial Wnt ligand secretion is required for adult hair follicle growth and regeneration. *J Invest Dermatol* 133:31–41.
53. Brownell I, Guevara E, Bai CB, Loomis CA, Joyner AL (2011) Nerve-derived sonic hedgehog defines a niche for hair follicle stem cells capable of becoming epidermal stem cells. *Cell Stem Cell* 8:552–565.
54. Driskell RR, Giangreco A, Jensen KB, Mulder KW, Watt FM (2009) Sox2-positive dermal papilla cells specify hair follicle type in mammalian epidermis. *Development* 136: 2815–2823.
55. Hsu YC, Li L, Fuchs E (2014) Transit-amplifying cells orchestrate stem cell activity and tissue regeneration. *Cell* 157:935–949.
56. Zhang B, et al. (2016) Hair follicles' transit-amplifying cells govern concurrent dermal adipocyte production through sonic hedgehog. *Genes Dev* 30:2325–2338.
57. Paladini RD, Saleh J, Qian C, Xu GX, Rubin LL (2005) Modulation of hair growth with small molecule agonists of the hedgehog signaling pathway. *J Invest Dermatol* 125: 638–646.
58. Xue T, et al. (2011) Melanopsin signalling in mammalian iris and retina. *Nature* 479: 67–73.
59. Matynia A, et al. (2016) Peripheral sensory neurons expressing melanopsin respond to light. *Front Neural Circuits* 10:60.
60. Güler AD, et al. (2008) Melanopsin cells are the principal conduits for rod-cone input to non-image-forming vision. *Nature* 453:102–105.
61. Hatori M, et al. (2008) Inducible ablation of melanopsin-expressing retinal ganglion cells reveals their central role in non-image forming visual responses. *PLoS One* 3:e2451, and erratum (2008) 4, 10.1371/annotation/c02106ba-b00b-4416-9834-cf0f3ba49a37.
62. Botchkarev VA, Eichmüller S, Johansson O, Paus R (1997) Hair cycle-dependent plasticity of skin and hair follicle innervation in normal murine skin. *J Comp Neurol* 386: 379–395.
63. Paus R, Peters EM, Eichmüller S, Botchkarev VA (1997) Neural mechanisms of hair growth control. *J Investig Dermatol Symp Proc* 2:61–68.
64. Martin CM, Southwick EG, Maibach HI (1973) Propranolol induced alopecia. *Am Heart J* 86:236–237.
65. Zyluk A (2003) A new clinical severity scoring system for reflex sympathetic dystrophy of the upper limb. *J Hand Surg [Br]* 28:238–241.
66. Sato N, Leopold PL, Crystal RG (1999) Induction of the hair growth phase in postnatal mice by localized transient expression of Sonic hedgehog. *J Clin Invest* 104:855–864.
67. Plikus MV, et al. (2013) Local circadian clock gates cell cycle progression of transient amplifying cells during regenerative hair cycling. *Proc Natl Acad Sci USA* 110: E2106–E2115.
68. Al-Nuaimi Y, et al. (2014) A meeting of two chronobiological systems: Circadian proteins Period1 and BMAL1 modulate the human hair cycle clock. *J Invest Dermatol* 134:610–619.
69. Janich P, et al. (2011) The circadian molecular clock creates epidermal stem cell heterogeneity. *Nature* 480:209–214.
70. Bartness TJ, Song CK, Demas GE (2001) SCN efferents to peripheral tissues: Implications for biological rhythms. *J Biol Rhythms* 16:196–204.
71. Niijima A, Nagai K, Nagai N, Nakagawa H (1992) Light enhances sympathetic and suppresses vagal outflows and lesions including the suprachiasmatic nucleus eliminate these changes in rats. *J Auton Nerv Syst* 40:155–160.
72. Niijima A, Nagai K, Nagai N, Akagawa H (1993) Effects of light stimulation on the activity of the autonomic nerves in anesthetized rats. *Physiol Behav* 54:555–561.
73. Morrison SJ, Spradling AC (2008) Stem cells and niches: Mechanisms that promote stem cell maintenance throughout life. *Cell* 132:598–611.
74. Chi W, Wu E, Morgan BA (2013) Dermal papilla cell number specifies hair size, shape and cycling and its reduction causes follicular decline. *Development* 140:1676–1683.
75. Buscone S, et al. (2017) A new path in defining light parameters for hair growth: Discovery and modulation of photoreceptors in human hair follicle. *Lasers Surg Med* 49:705–718.
76. Bailes HJ, Lucas RJ (2013) Human melanopsin forms a pigment maximally sensitive to blue light (lambdamax approximately 479 nm) supporting activation of G(q/11) and G(i/o) signalling cascades. *Proc Biol Sci* 280:20122987.
77. Knox SM, et al. (2013) Parasympathetic stimulation improves epithelial organ regeneration. *Nat Commun* 4:1494.
78. Katayama Y, et al. (2006) Signals from the sympathetic nervous system regulate hematopoietic stem cell egress from bone marrow. *Cell* 124:407–421.
79. Lucas D, Battista M, Shi PA, Isola L, Frenette PS (2008) Mobilized hematopoietic stem cell yield depends on species-specific circadian timing. *Cell Stem Cell* 3:364–366.
80. Chen SK, et al. (2013) Apoptosis regulates ipRGC spacing necessary for rods and cones to drive circadian photoentrainment. *Neuron* 77:503–515.
81. Conboy IM, et al. (2005) Rejuvenation of aged progenitor cells by exposure to a young systemic environment. *Nature* 433:760–764.
82. Templeton JP, Geisert EE (2012) A practical approach to optic nerve crush in the mouse. *Mol Vis* 18:2147–2152.
83. Parrilla-Reverter G, et al. (2009) Effects of different neurotrophic factors on the survival of retinal ganglion cells after a complete intraorbital nerve crush injury: A quantitative in vivo study. *Exp Eye Res* 89:32–41.
84. Pfeiffenberger C, et al. (2005) Ephrin-As and neural activity are required for eye-specific patterning during retinogeniculate mapping. *Nat Neurosci* 8:1022–1027.
85. Kostrzewa RM, Jacobowitz DM (1974) Pharmacological actions of 6-hydroxydopamine. *Pharmacol Rev* 26:199–288.
86. Blecher SR (1986) Anhidrosis and absence of sweat glands in mice hemizygous for the Tabby gene: Supportive evidence for the hypothesis of homology between Tabby and human anhidrotic (hypohidrotic) ectodermal dysplasia (Christ-Siemens-Touraine syndrome). *J Invest Dermatol* 87:720–722.
87. Morgan DA, Despas F, Rahmouni K (2015) Effects of leptin on sympathetic nerve activity in conscious mice. *Physiol Rep* 3:e12554.
88. Chang CY, et al. (2013) NFIB is a governor of epithelial-melanocyte stem cell behaviour in a shared niche. *Nature* 495:98–102.
89. Lin SJ, et al. (2013) Topology of feather melanocyte progenitor niche allows complex pigment patterns to emerge. *Science* 340:1442–1445.